Effect of amino acid addition on the micelle formation of surface active ionic liquid, 1-tetradecyl-3-methylimidazolium bromide in aqueous solution

Mabel Rojas,[a] Zsombor Miskolczy,[b] László Biczók[b] and Paulina Pavez*[a]

[a] *Facultad de Química, Pontificia Universidad Católica de Chile, Casilla 306, Santiago 6094411, Chile*

[b] *Institute of Materials and Environmental Chemistry, Research Centre for Natural Sciences, Hungarian Academy of Sciences, P.O. Box 286, 1519 Budapest, Hungary*

Author Information

∗Corresponding authors. Tel.: +56-02-23541743; fax: +56-02-26864744; e-mail: ppavezg@uc.cl

Present address: Facultad de Química, Pontificia Universidad Católica de Chile, Av. Vicuña Mackenna 4860, Santiago 6094411, Chile.

Abstract.

The effect of three amino acids on the self-organization of surface active ionic liquid, 1-tetradecyl-3-methyl imidazolium bromide, [$C_{14}mim^+$][Br^-] was studied in neutral and basic aqueous solution. The critical micelle concentrations (cmc) were determined by surface tension, conductivity, steady-state fluorescence measurements and isothermal titration calorimetry (ITC). Thermodynamics parameters of micellization (ΔG^0_{mic}, ΔH^0_{mic} and ΔS^0_{mic}) were measured by ITC.

The cmc values decrease in presence of all amino acids used in this study. The most substantial effect was observed in presence of L-tryptophan at pH 12, due to the electrostatic and $\pi-\pi$ interactions with the imidazolium headgroup of the surfactant. Always entropy-driven micellization occurred. Both the enthalpy and entropy changes upon association to micelles increased when the pH was enhanced from 7 to 12.

^{1}H NMR measurements demonstrated that among the used amino acids L-tryptophan interacts most strongly with the headgroup of surfactant cation.

1. Introduction

Ionic liquids (ILs) have received much attention in the last decades due to their unique physicochemical characteristics, such as negligible vapor pressures, non-flammability, and easy recyclability, among others.[1] Due to their advantageous properties, ILs has been used as solvents in many fields including preparation of novel nanomaterials, organic synthesis, homogeneous catalysis, and electrochemistry.[2,3] In addition, the homologues containing a long hydrophobic alkyl chain can self-assemble to various types of aggregates in aqueous solutions such as micelles,[4-6] vesicles,[7] lyotropic liquid crystals (LLCs)[8-10] and gels.[11] These ILs, generally named as surface active ionic liquids (SAILs), have been extensively studied. It has been demonstrated that the length of alkyl chain, type of head of group and the nature of counterions affects the self-aggregation,[12-14] leading to modification in cmc, size, shape, and aggregation number (N_{agg}); among others.[14]

The most frequently studied SAILs are 1-alkyl-3-methylimidazolium ($[C_nmim^+]$) cations containing halide (Br^-; Cl^-) or fluorinated $[BF_4^-]$; $[PF_6^-]$; bis(trifluoromethylsulfonyl)imide ($[NTf_2^-]$) anions.[15-17] The alkyl chain length of $[C_nmim^+]$ and the nature of the counterions affect both the micellization properties and micelle shape.[15,17,18] For example, only $[C_nmim^+]Cl^-$ with n >8 form aggregates in solution and when Cl^- was replaced by $[NTf_2^-]$ or $[PF_6^-]$ anions, no micelle formation was detected.[15] Moreover, other types of SAILs with varied ring type of the cations, such as alkylpyridinium ($[C_nPy^+]$), alkylmethylpyrrolidinium ($[C_nmPyrr^+]$), alkylmethylpiperidinium ($[C_nmpip^+]$), morpholinium ($[C_nMorph^+]$), have been reported.[19-22] Wang et al. found that the hydrophobicity and steric hindrance of cations had very weak effects on the morphology, but played an important role in the control of the size of aggregates.[19] In addition, other parameters such as temperature and the presence of inorganic or organic additive exerted a significant effect on the self-aggregation behavior of a number of surfactants.[23-26] Structural and thermodynamic studies have been performed on surfactant-water systems including the effect of additives on micellization.[24,27] The addition of salicylate ions to aqueous solution of the cationic surfactant alkyltrimethylammonium type $[RTA^+]$ lead to considerable changes in the properties of self-aggregation. These results have been explained by the peculiar manner of salicylate binding to the micelles. Due to its amphiphilic character, the

salicylate inserts its benzene ring into the hydrophobic part of the micelle.[28] In contrast, addition of glutamine, histidine and methionine barely influenced the cmc of sodium dodecyl benzene sulfonate and dodecyltrimethylammonium bromide.[24]

Previous studies revealed that surfactants are usually toxic which hinders their applications in many fields.[29] Therefore, the syntheses and study of more eco-friendly surfactants composed of biocompatible constituents represents an important challenge.

Recent studies on the counterion effect on the physicochemical characteristics of a new enviromental friendly surfactant, ethane-1,2-diyl bis(N,N-dimethyl-N-tetradecyl-ammoniumacetoxy) dichloride found that the rise of anthranilate or tosylate concentration brought about substantial reduction in cmc values and surfactant headgroup area which was accompanied with a significant growth of aggregation number because of the incorporation of these organic anion into the palisade layer of micelles.[23] The only electrostatically bound inorganic anions exerted smaller effect.

The main goal of the present work was to reveal how the presence of L-alanine (L-Ala), L-phenylalanine (L-Phe) and L-tryptophan (L-Trp) amino acids modified the micellization properties of 1-tetradecyl-3-methylimidazolium bromide [$C_{14}mim^+$][Br^-] in aqueous solution (Figure 1). Experiments were carried out at pH 7 and pH 12, where zwitterionic and anionic forms of amino acids dominate, respectively. Conductivity, surface tension (ST), NMR, and steady-state fluorescence spectroscopic measurements combined with isothermal titration calorimetry (ITC) provide a comprehensive view on the interaction of amino acids with [$C_{14}mim^+$][Br^-] micelles.

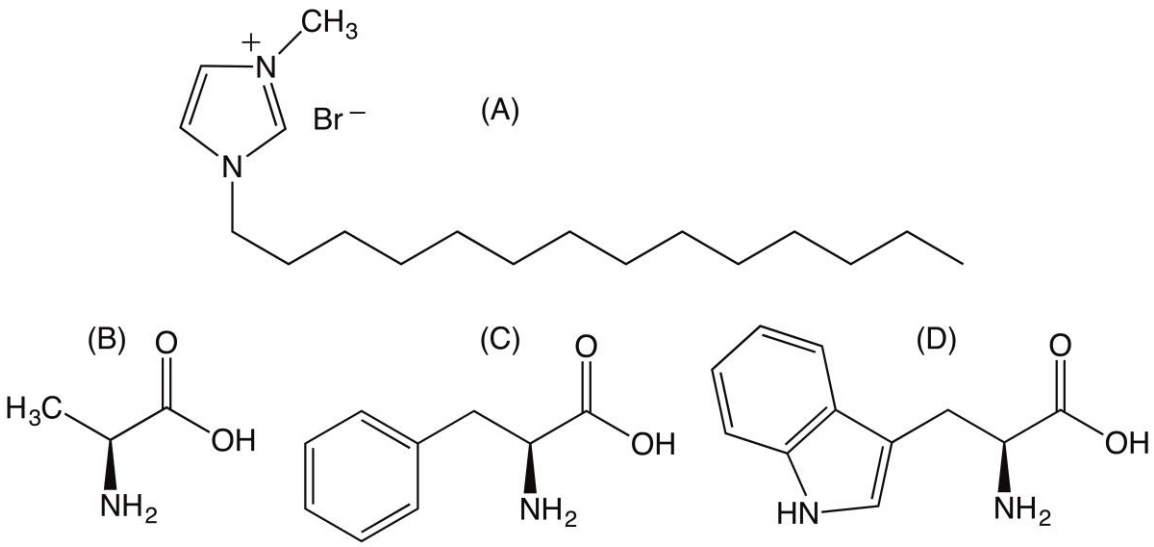

Figure 1. Structure of (A) 1-tetradecyl-3-methylimidazolium bromide ([$C_{14}mim^+$][Br^-]); (B) L-alanine (L-Ala); (C) L-phenylalanine (L-Phe) and (D) L-tryptophan (L-Trp).

2. Experimental Section

2.1 Materials.

Commercially available reagents and solvents were used as received from Sigma Aldrich unless otherwise specified. Doubly distilled deionized water was obtained from a Millipore Milli-Q water purification system (Millipore). 1-Tetradecyl-3-methylimidazolium bromide; [$C_{14}mim^+$][Br^-] was synthesized according to a procedure reported in the literature[30] and dried in vacuum for at least 48 h at 333 K before use. Solutions were prepared with doubly distilled Millipore Milli-Q water.

2.2 Methods.

2.2.1. Surface tension measurements (ST).

ST measurements were carried out at two different experimental conditions; pH 7 and pH 12, using a Krüss manual tensiometer K20 by the Du Noüy ring method. Prior to each experiment, the tensiometer was calibrated at 298 K with doubly distilled Millipore Milli-Q water. The temperature was controlled at 298 ± 0.1 K using a thermostatic bath. All measurements were repeated at least 5 times.

2.2.2 Conductivity measurements.

The samples were equilibrated at 298 ± 0.1 K in a thermostatic bath, and then conductivity measurements were performed on a Consort C832 apparatus, which was calibrated with KCl solutions. The cmc was calculated as the intersection point of the two linear regimes in the conductivity-concentration graph. The degree of counter ion binding was calculated using the following equation $\beta = 1 - \alpha$, where α is the degree of ionization derived from the ratio of the slopes between the two linear fragments of the conductivity curves. All measurements were made at pH 7 and were repeated 3 times. The small conductivity of water was always subtracted from the measured data.

2.2.3 Steady-state fluorescent measurements.

Steady-state fluorescence spectra were taken on a Jobin-Yvon Fluoromax-P photoncounting spectrofluorometer. The selected excitation wavelength (λ_{ex}) was 335 nm and the emission spectra were scanned from 350 to 500 nm. Pyrene (2.0 μM) and N-tetradecylpyridinium bromide ($[C_{14}Py^+][Br^-]$) (0 – 0.25 mM) were used as florescence probe and quencher, respectively. An appropriate volume of pyrene solution in methanol was introduced into a volumetric flask, and the solution was purged with a stream of nitrogen. Intensities of first (I_1) and third (I_3) vibronic bands in the pyrene emission spectra located at 373 and 384 nm, respectively, were used to obtain the cmc value from the surfactant concentration dependence of the I_1/I_3 ratio. All measurements were performed at pH 7 and pH 12 at 298 K and were repeated at least three times.

2.2.4 Isothermal titration calorimetry.

ITC measurements were executed using a MicroCal VP-ITC microcalorimeter at pH 7 and pH 12. 10 μL volumes of 3.4 mM $[C_{14}mim^+][Br^-]$ aqueous solution were injected from the computer-controlled microsyringe at an interval of 180 s into the cell (volume = 1.4569 mL) containing 50 mM of amino acid solutions, while stirring at 450 rpm. Triplicate measurements were taken for each of the experimental points.

2.2.5 NMR measurements.

The 400 MHz Bruker AC-NMR spectrometer was utilized to probe ^{1}H NMR shifts of the signals of [$C_{14}mim^{+}$][Br^{-}] surfactant upon addition of amino acids in deuterated water (D_2O) relative to tetramethylsilane internal standard. The acquisition of spectra and its analysis were handled by MestReNova software. All experiments were performed at pH 7 and 12 at 298 ± 0.1 K.

3. Results and Discussion

3.1 Characterization of the self-aggregation properties of [$C_{14}mim^{+}$][Br^{-}].

We have examined the effect of some AA such as L-Ala, L-Phe and L-Trp on the self-aggregation behavior of the surfactant [$C_{14}mim^{+}$][Br^{-}] in aqueous solution at 298 K. In order to investigate the formation of micelles in water, the cmc of [$C_{14}mim^{+}$][Br^{-}] in presence of AAs were measured in aqueous solution at pH 7 and pH 12 by four techniques such as; surface tension, conductivity, steady-state fluorescence, and ITC techniques. Furthermore, thermodynamics and surface parameters were determined. The results will be discussed in the following paragraphs in detail.

3.1.1 Determination of cmc values.

Surface tension measurements.

Figure 2 shows the variation of the ST (γ) as a function of the logarithm of [$C_{14}mim^{+}$][Br^{-}] concentration in presence of 50 mM AA at pH 7 and pH 12; respectively. The experimental data at pH 7 and pH 12 are summarized in Supporting Information, in Table S1 and S2, respectively. As we can see in Figure 2, after the initial gradual diminution, a break point is observed which corresponds to the cmc. The cmc values obtained to [$C_{14}mim^{+}$][Br^{-}] in absence and in presence of AAs at both pHs are show in Table 1.

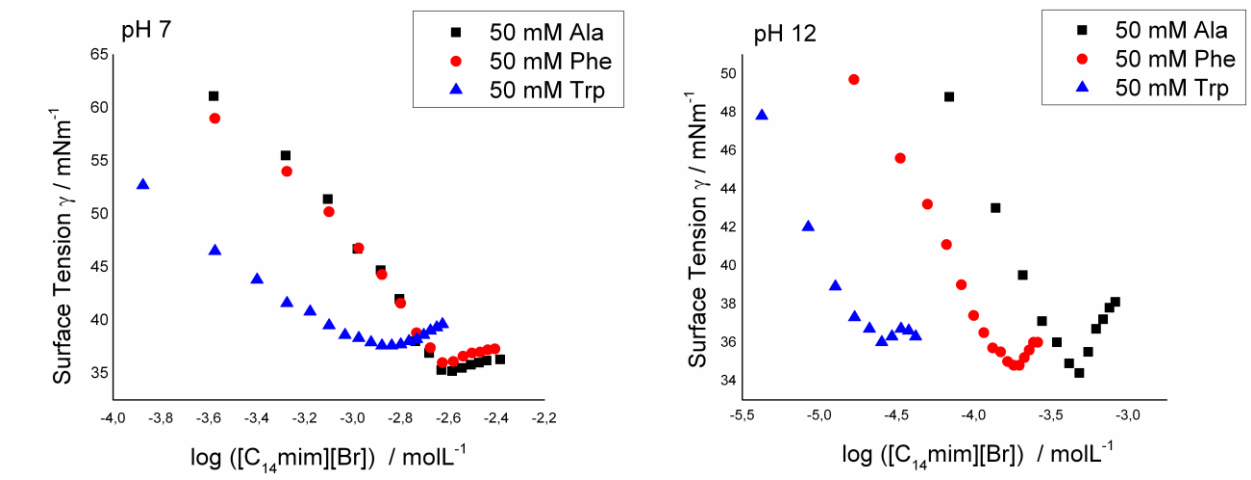

Figure 2. Surface tension *vs* log C isotherms for [$C_{14}mim^+$][Br^-] aqueous solution in the presence of 50 mM AAs, at pH 7 and pH 12.

Conductivity measurements.

Two readily distinguishable linear correlations appear when the specific conductivity (κ) is plotted as a function of [$C_{14}mim^+$][Br^-] concentration in aqueous solution in presence of AAs at pH 7 (see Figure 3). At low surfactant concentrations, the growth of κ is attributed to the increase of the number of free [$C_{14}mim^+$] and [Br^-] ions, whereas the break in the change of the slope arises from the onset of micelle formation. Above cmc, the binding of a fraction of the counterions to the micellar surface and the low mobility of micelles leads to a smaller slope for the concentration dependence of κ.[31] The larger slope above cmc in the presence of L-Trp may indicate smaller extent of counterion association with micelle and/or smaller micelle size. The intersection of the two linear correlations, which corresponds to the cmc, appears at lower surfactant concentration in L-Trp solution than in the case of the other AAs. The parameters calculated from conductivity experiments are given in Table S3 in Supporting Information. The degree of counterion binding (β) can be estimated from the ratio of the slopes[32] and indicates the amount of anions on the surface of the micelles. Because of the high Na^+ and OH^- concentrations, conductivity measurement does not provide information on the micellization at pH 12. The cmc and β values obtained for [$C_{14}mim^+$][Br^-] in presence of AAs at pH 7 are show in Table 1.

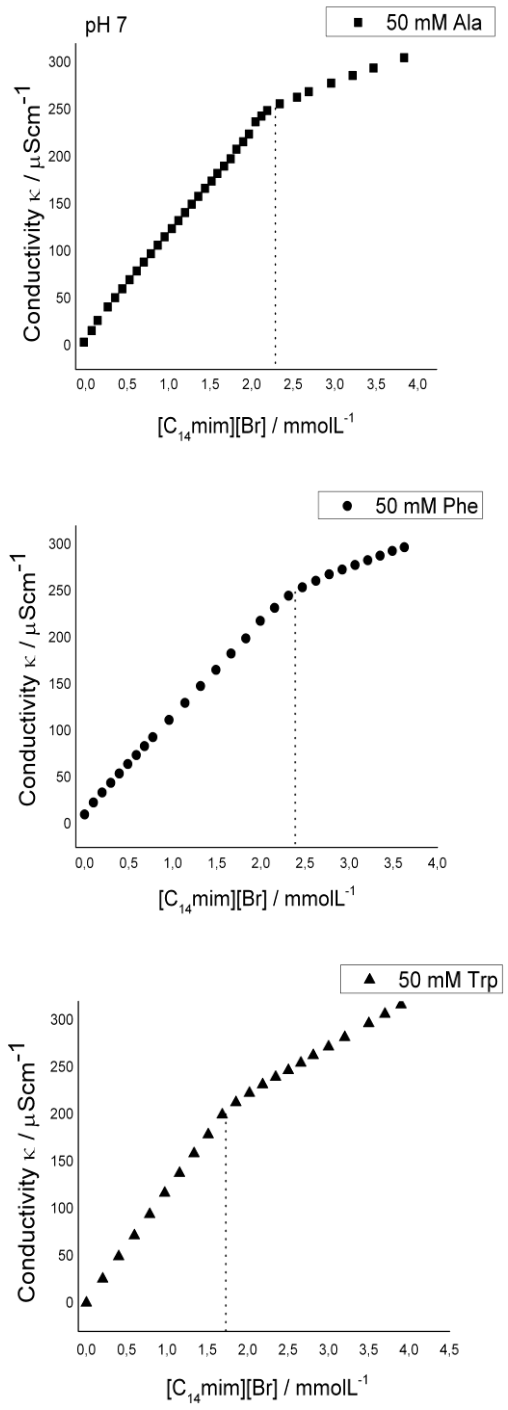

Figure 3. Specific conductance *vs* concentration isotherms for $[C_{14}mim^+][Br^-]$ aqueous solution at pH 7, in presence of 50 mM of AA.

Steady-state fluorescence measurements.

The alteration of the steady-state fluorescence spectrum of pyrene probe was also used to determine the cmc values of $[C_{14}mim^+][Br^-]$ in presence of each AA. The pyrene emission has characteristic five vibronic bands in the region from 370 to 425 nm (see Figure S1 in Supporting Information). When pyrene is dissolved in surfactant, the intensity of the first band decreases due to less polar microenvironment compared with water, while the third band is not sensitive to the surroundings of the excited molecule. Thus, the ratio of the intensities of the first to third bands (I_1 /I_3) is useful to probe the micropolarity. In addition, when the ratio (I_1/I_3) is correlated with the surfactant concentration, break point corresponds to the cmc value.

The plots showing the variation of the I_1/I_3 ratio with the concentration of $[C_{14}mim^+][Br^-]$ in aqueous solution and in presence of each AA at pH 7 and pH 12 are shown in Figure 4. The variations of the I_1/I_3 ratio calculated are presented in Table S4 and S5 in Supporting Information. The overlap between the emission of pyrene and L-Trp thwarted the determination of cmc by fluorescence method in the presence of this AA.

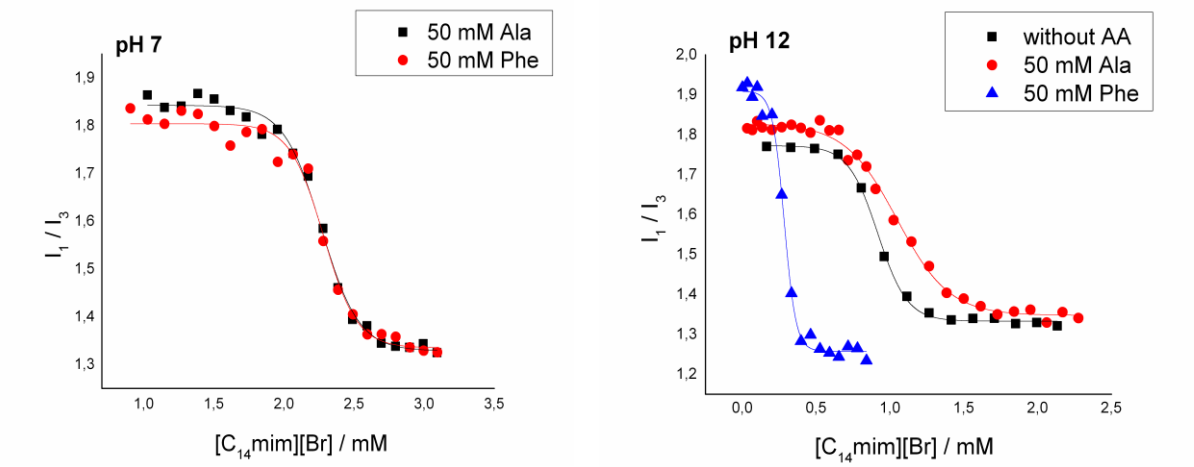

Figure 4. Variation of the I_1/I_3 ratio with the concentration of aqueous solution of $[C_{14}mim^+][Br^-]$; i) pH 7: in presence of 50 mM of L-Ala and L-Phe, ii) pH 12: in absence and in presence of 50 mM of L-Ala and L-Phe, at 25ºC.

Isothermal titration calorimetry.

Finally, ITC measurements were performed in order to determine the cmc values of $[C_{14}mim^+][Br^-]$ and to obtain the thermodynamic parameters of micellization in presence of each AA at pH 7 and pH 12. Figures 6 show the enthalpograms of dilution in presence of L-Ala, L-Phe and L-Trp at pH 7, respectively. The results of analogous experiments at pH 12 are presented in Figures 7. These profiles can typically be described in terms of three different regions. At low concentrations of the surfactant a relatively large and constant enthalpy change (ΔH) is observed due to the complete dissociation of the micelles of the titrant solution. The second region is characterized by a sharp and decreasing endothermic effect indicating that the only a fraction of the injected micelles disintegrate. In the third concentration range no disaggregation occurs because micelles exit in the titrant solution. The enthalpy change of demicellization (ΔH_{demic}) was determined as described by Blume and coworkers.[33] The alteration of the dilution enthalpy *vs* concentration of $[C_{14}mim^+][Br^-]$ in the presence of each AA at pH 7 and pH 12 are shown in Table S6 and S7, respectively in Supporting Information.

The cmc values were obtained from the inflection points, as determined from the first derivative of the enthalpogram, as shown in Figure S4 in Supporting Information, for $[C_{14}mim^+][Br^-]$ in aqueous solution in presence of L-Ala, L-Phe and L-Trp at pH 7; respectively. Similarly, the cmc values at pH 12 were obtained from the inflection points. Figures S5 in Supporting Information show the first order differential of the enthalpy profile curves for $[C_{14}mim^+][Br^-]$ in aqueous solution in absence of AA and in presence of L-Ala, L-Phe and L-Trp at pH 12.

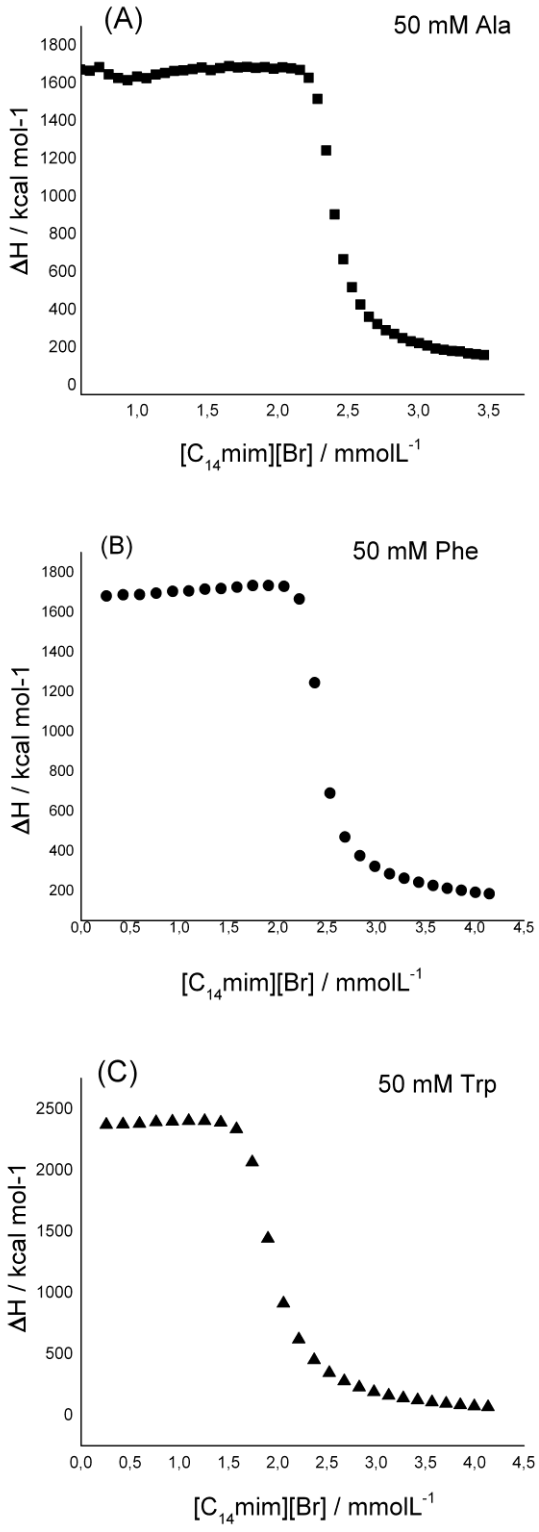

Figure 6. Raw titration data from ITC in $kcalmol^{-1}$; each peak corresponds to a single injection of $[C_{14}mim^{+}][Br^{-}]$ aqueous solution, in presence of each AA, at pH 7.

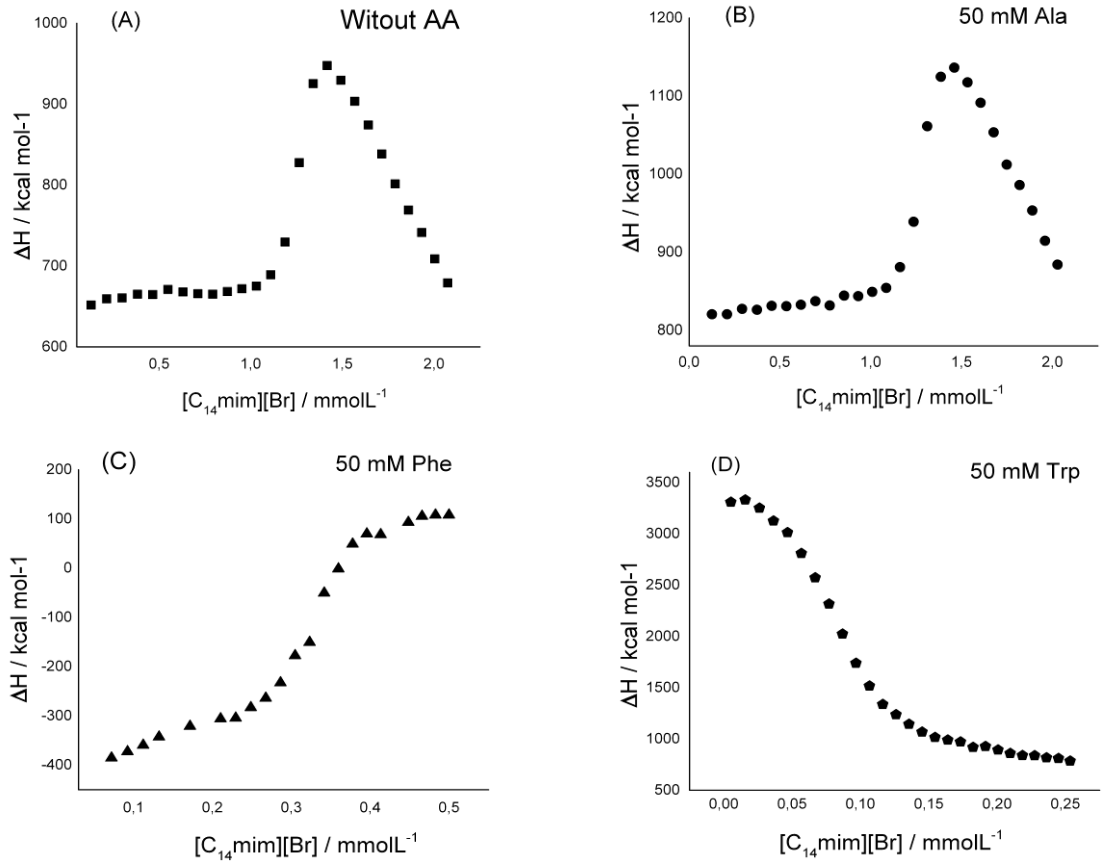

Figure 7. Raw titration data from ITC in $kcalmol^{-1}$; each peak corresponds to a single injection of $[C_{14}mim^{+}][Br^{-}]$ aqueous solution, in presence of each AA, at pH 12.

The cmc values of $[C_{14}mim^{+}][Br^{-}]$ in presence of the AA at pH 7 and pH 12, obtained by four independent methods are summarized in Table 1.

Table 1. Cmc of $[C_{14}mim^{+}][Br^{-}]$ with different amino acids (50 mM), at two pHs. Each measurement was made in triplicate.

Amino Acid	pH	Surface Tension				Conductivity		ITC	Fluoresce	
		CMC / mM	Π_{cmc} mNm^{-1}	Γ_{max} / (10^4 mol/m^2)	A_{min} / nm^2	CMC / mM	β	CMC / mM	CMC / mM	N_{agg}
-	7	2.50[34]	33.8[34]	18	0.92	2.50[34]	0.76[34]	2.50[34]	2.50[34]	59[34]
L-Ala	7	2.45 ± 0.02	34.7	15	1.09	2.21 ± 0.04	0.72	2.43 ± 0.04	2.26 ± 0.01	49
L-Phe	7	2.36 ± 0.02	32.2	10.7	1.56	2.33 ± 0.03	0.65	2.47 ± 0.07	2.26 ± 0.03	57
L-Trp	7	1.24 ± 0.02	31.1	0.66	8.6	1.76 ± 0.02	0.56	1.90 ± 0.04	**	**
-	12	0.61 ± 0.01	35.7	4.10	26.2	***	***	1.34 ± 0.02	0.91 ± 0.01	63
L-Ala	12	0.48 ± 0.01	32.4	7.44	2.40	***	***	1.31 ± 0.02	1.05 ± 0.02	58
L-Phe	12	0.18 ± 0.01	34.4	2.19	7.57	***	***	0.322 ± 0.003	0.28 ± 0.01	55
L-Trp	12	0.025 ± 0.002	35.6	1.92	8.64	***	***	0.075 ± 0.002	**	**

** It was not possible to measure cmc by fluorescence technique due to L-Trp fluorescence

*** It was not possible to obtain information by conductivity techniques due to the high background conductivity at pH 12.

As we can see in Table 1, the cmc values found to [$C_{14}mim^+$][Br^-] by different techniques (surface tension, conductivity, ITC and fluorescence) in general agree closely with each other. Nevertheless, ITC measured cmc values determined for [$C_{14}mim^+$][Br^-] at pH 12 in absence of AA and in presence of L-Ala and L-Phe are higher, even values greater than double was observed in some cases. A similar behavior was observed by Sastry *et al*, when the critical aggregation concentration (cac) values determined by ST and ITC were compared.[35] They reported important differences of cac values for some SAILs such as 1-dodecyl-1-methylpiperidinium acetylsalicylate [$C_{12}mpip^+$][$AcSa^-$] and 1-dodecyl-1-methyl piperidinium chloride [$C_{12}mpip^+$][Cl^-]. ITC measurements provide different cmc because it reflects not only the aggregation but also the changes in the thermodynamic functions associated with microstructural changes during the aggregation process.[36]

On the other hand, the values of cmc in the Table 1 at pH 7 and pH 12 show differences among them. A larger effect on the cmc values was observed at pH 12 in presence of each AA. These results are in accordance with the substantial electrostatic interactions between anionic forms of each AA (at pH 12) with the cationic surfactant.

At pH 7, slight interactions of the L-Ala with the surfactant [$C_{14}mim^+$][Br^-] were observed, compared with the effect found when L-Trp was the additive. These results could be explained due to the presence of a hydrophobic moiety on the L-Trp (indole group), that interacts strongly with the micellar interface of the [$C_{14}mim^+$][Br^-], favoring micelle

formation at a lower cmc value. Interestingly, in the case of pH 12, even higher effect was observed in the presence of each AA. The decrease in the cmc value follows the tendency: absence AA > L-Ala > L-Phe > L-Trp. Two effects contribute to this trend: (i) hydrophobic interactions between the surfactant and the aromatic moiety of AA and (ii) the electrostatic attraction between [$C_{14}mim^+$] and the anionic form of AA.

3.1.2 Determination of surface parameters

On the other hand, other surface active parameters could be determined for a surfactant when the self-aggregation properties are determined by a ST technique.[37] In this context, the area per adsorbed molecule at the air/water interface (A_{min}), the surface excess concentration (Γ_{max}), and the surface pressure (π_{CMC}) were calculated. The equations used to calculate the surface-active parameters mention above are given in Supporting Information (see equations S1, S2 and S3). The results are shown in Table 1.

Interestingly, the A_{min} and Γ_{max} values (see Table 1) in general, decrease in presence of AAs, at pH 12. These results could be explain due to that, L-Trp induce a better compaction of the surfactant at the interface and due to the electrostatic interaction between the surfactant [$C_{14}mim^+$][Br^-] and the AAs.[38]

In addition, the steady-state fluorescence of pyrene probe was utilized to determine the aggregation number (N_{agg}) of [$C_{14}mim^+$][Br^-] surfactant under different experimental conditions by static luminescence quenching method proposed originally by Turro and Yekta.[39] The logarithm of the pyrene fluorescence intensity ratios at a specific wavelength (I_0/I) in the absence and in the presence of quencher provides a linear correlation with the concentration of quencher and from the slope; N_{agg} can be determined. See equation S4 in Supporting Information.[38,39] As an example, Figure 5 shows the change in pyrene fluorescence emission spectra as a function of the concentration of the quencher for the aqueous solution of [$C_{14}mim^+$][Br^-] (25 mM), in the presence of L-Phe, at pH 12.

Figures S2 to S3 in Supporting Information show the same behaviour at pH 7 and pH 12 in absence of AA and in presence of L-Ala and L-Phe; respectively.

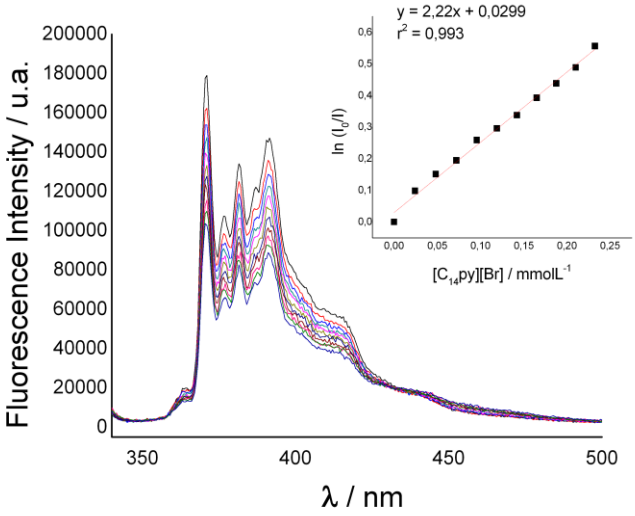

Figure 5. Plots of changes in the pyrene fluorescence spectra as a function of the concentration of quencher, N-tetradecylpyridinium bromide ($[C_{14}py^+][Br^-]$), using 25 mM $[C_{14}mim^+][Br^-]$) in the presence of 50 mM L-Phe at pH 12. The inset shows the plot of $\ln(I_0/I)$ for pyrene *vs* the concentration of the quencher, $[C_{14}py^+][Br^-]$, for the aqueous solution of $[C_{14}mim^+][Br^-]$ (25 mM) in the presence of 50 mM L-Phe at pH 12.

The values of the N_{agg} calculated for the aggregates formed from $[C_{14}mim^+][Br^-]$ at both pHs in absence and in presence of AA are summarized in Table 1. As we can see, there is no tendency in neutral solution, but a clear trend appears at pH 12. As the size of the AA increase, there is a decrease in the N_{agg}. The decrease in the N_{agg} value follows the trend: without AA > L-Ala > L-Phe.

3.1.3 Determination of thermodynamics parameters.

Additionally, thermodynamic parameters, namely, Gibbs free energy (ΔG^0_{mic}), enthalpy (ΔH^0_{mic}), and entropy of micellization (ΔS^0_{mic}), have been obtained from ITC measurements. ITC is a label-free direct measurement of the heat evolved or absorbed during the aggregation process. Figure 6 at pH 7 and figure 7 at pH 12, shown the experimental data of the changes in heats of dilution as a function of the concentration was fitted by an independent site-binding model based on the sigmoidal Boltzman, procedure to calculate the ΔH_{demic}. Since micellization is a reversible process, the enthalpy of demicellization is directly correlated to the enthalpy of micellization.

The equations used to calculate the thermodynamic parameters mention above are given in Supporting Information, see equation S5 and S6.[40,41] The summary of the thermodynamic parameters of micellization for [$C_{14}mim^+$][Br^-] in absence and in presence of each AA, at pH 7 and pH 12 are given in Table 2.

The ΔG^0_{mic} is negative in every case for the micellization of [$C_{14}mim^+$][Br^-] in aqueous solution in the presence of the AA at two different pHs. This indicates the spontaneous nature of micellization of the surfactant. The negative value of ΔH^0_{mic} at pH 7 and in the presence of L-Trp at pH 12 suggest the exothermic nature of micellization, while positive values in absence of AA, with L-ala and L-Phe at pH 12, indicate that the micellization process are endothermic. The values of ΔS^0_{mic} calculated are positive and always entropy-driven micellization occurs.

A comparison of the thermodynamic parameters of micellization of the [$C_{14}mim^+$][Br^-] in the absence of AA and in the presence of L-Trp reveals that the free energy and enthalpy of micellization are more negative in presence of L-Trp than in absence of AA. This indicates that the L-Trp facilities the micellization process more favorably both at pH 7 and at pH 12.

Table 2. Thermodynamics parameters of micellization obtain from ITC for [$C_{14}mim$][Br] with amino acids.

Amino acid	**pH**	**ΔG^0_{mic} / kJ mol^{-1}**	**ΔH^0_{mic} / kJ mol^{-1}**	**$T\Delta S^0_{mic}$ / kJ mol^{-1}**
-	7	-24.79	-5.72	19.07
L-Ala	7	-24.89	-5.82	19.07
L-Phe	7	-24.77	-6.02	18.75
L-Trp	7	-25.48	-9.40	16.08
-	12	-26.34	1.45	27.78
L-Ala	12	-26.4	1.61	28.01
L-Phe	12	-29.74	1.77	31.51
L-Trp	12	-33.65	-7.46	26.19

3.1.4 Electrostatic interaction by NMR techniques.

Finally, and in order to shed more light on the interaction between [$C_{14}mim^+$][Br^-] with the additives at pH 7 and pH 12, ^{1}H NMR technique was used. It provides information about average position of AA within the micellar aggregates.[23]

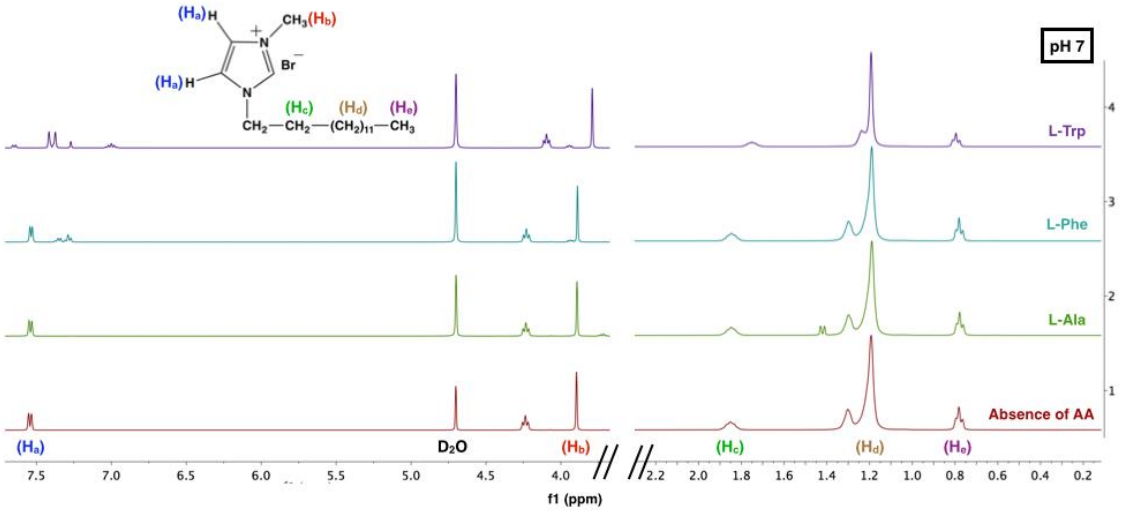

Figure 5. ^{1}H NMR spectrum of [$C_{14}mim^+$][Br^-] surfactant at pH 7; in absence and in presence of each AA.

Figures 5 and 6 show the ^{1}H NMR spectrum of [$C_{14}mim^+$][Br^-] surfactant, in absence and in presence of AA, at pH 7 and pH 12 respectively. The concentration of [$C_{14}mim^+$][Br^-] was 80 times higher than cmc (200 mM). The Figures 5 and 6 show that the micellar core protons (called as H_c, H_d and H_e) of [$C_{14}mim^+$][Br^-] surfactant in the absence of AA are highly shielded and therefore they are at low chemical shifts (δ) values. In addition, protons near the head group (these protons are called H_a and H_b) resonate at higher δ values, due to deshielding effect caused by the positive charge of the imidazolium group. On the other hand, we can observe in Figure 5 that there is not a significant effect on the chemical shifts of the protons mention above after addition of L-Ala and L-Phe, suggesting a poor interaction between the surfactant and zwitterionic form of both AA. Nevertheless, when L-Trp is added to [$C_{14}mim^+$][Br^-] solution, the signals of H_a and H_b protons are shifted upfield (H_a from 7.54 to 7.39 ppm and H_b from 3.90 to 3.79 ppm). These results could explain the trend of the cmc values found to [$C_{14}mim^+$][Br^-] in absence and presence of each AA. As mentioned above, small effect was observed in the cmc values when L-Ala and L-Phe were

used as bio-additive, but a substantial decrease of cmc was observed in presence of L-Trp, where cmc decreased almost to half.

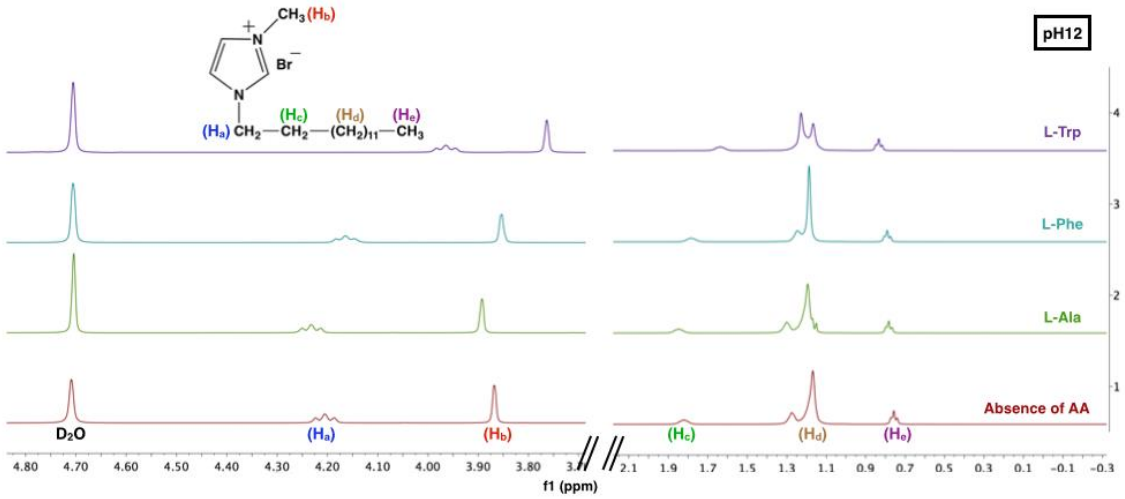

Figure 6. ^{1}H NMR spectrum of [C_{14}mim^{+}][Br^{-}] surfactant, in absence and in presence of each AA, at pH 12.

Figure 6 shows the effect after addition of each AA used in this study at pH 12 when all AAs are in the anionic form. There is not a significant effect on the chemical shifts of the core protons (H_c- H_e) after addition of L-Ala, L-Phe and L-Trp. Nevertheless, Figure 6 shows effect on chemical shifts of protons near the head group (H_a and H_b) after addition of L-Ala and L-Phe, which was not observed at pH 7. In addition, the effect on δ values of protons H_a and H_b is even higher when L-Trp is added to [C_{14}mim^{+}][Br^{-}] solution. (H_a from 4.20 to 3.96 ppm and H_b from 3.87 to 3.76 ppm).

This different behavior at pH 12 can be explained by the electrostatic attraction between the cationic head group of [C_{14}mim^{+}][Br^{-}] and the anionic form of AA. (Table S8 and S9 in Supporting Information, show all the chemical shifts (δ) values for H_a-H_e at pH 7 and 12; respectively).

Considering the NMR results mentioned above at pH 7 and 12, we conclude that the anionic form interacts more than the zwitterionic form of each AA. Besides, the chemical shifts of H_a and H_b shown in Figures 5 and 6 also indicate that AA interacts mainly with the head group of [C_{14}mim^{+}][Br^{-}].

4. Conclusion

The micellization behaviour and thermodynamic properties of $[C_{14}mim^+][Br^-]$ in aqueous solution at pH 7 and 12 were determined in the absence and in the presence of AAs such as L-alanine, L-phenylalanine and L-tryptophan.

The critical micellar concentrations were determined by four independent methods, namely, surface tension, conductivity, steady state fluorescence, and isothermal titration calorimetry measurements. The cmc values, obtained by different techniques, closely agreed. However, ITC measurements at pH 12 showed some cmc values higher compared with the other methods.

On the other hand, the greatest effect on the cmc values was observed at pH 12 for all amino acids, there was a decrease in the cmc values at this experimental condition. Nevertheless, the greatest decrease in the cmc value was in the presence of L-Trp, at pH 12. These results could be explained due to the presence of a hydrophobic moiety on the L-Trp, that can interact strongly with the micellar interface of the $[C_{14}mim^+][Br^-]$, favoring micelle formation at a lower cmc value.

Moreover, other surface parameters, such as; A_{min}, Γ_{max} and π_{CMC}, were determined from surface tension. Besides, steady state fluorescence techniques were used to determine the N_{agg} of $[C_{14}mim^+][Br^-]$ in presence of each AA. There is no tendency in neutral solution, but at pH 12 there are a clear trend. The N_{agg} decrease from without AA > L-Ala > L-Phe, and could be attributed to the size of the additive.

In order to understand the interaction between $[C_{14}mim^+][Br^-]$ with AA at pH 7 and pH 12, ^{1}H NMR technique was used. It was found that the anionic forms interact more than the zwitterionic forms of each additive. This result was explained by the electrostatic interaction between the cationic head group of $[C_{14}mim^+][Br^-]$ and the anionic form of AA.

Acknowledgements

References

(1) Hallett, J. P.; Welton, T. *Chem Rev* **2011**, *111*, 3508.
(2) Welton, T. *Coordin Chem Rev* **2004**, *248*, 2459.

(3) P. Wasserscheid, T. W. *Ionic Liquids in Synthesis*, 2003.
(4) Law, G.; Watson, P. R. *Langmuir* **2001**, *17*, 6138.
(5) Bhadani, A.; Singh, S. *Langmuir* **2009**, *25*, 11703.
(6) Zhao, Y.; Gao, S. J.; Wang, J. J.; Tang, J. M. *J Phys Chem B* **2008**, *112*, 2031.
(7) Yuan, J.; Bai, X. T.; Zhao, M. W.; Zheng, L. Q. *Langmuir* **2010**, *26*, 11726.
(8) Zhang, G. D.; Chen, X. A.; Xie, Y. Z.; Zhao, Y. R.; Qiu, H. Y. *J Colloid Interf Sci* **2007**, *315*, 601.
(9) Inoue, T.; Dong, B.; Zheng, L. Q. *J Colloid Interf Sci* **2007**, *307*, 578.
(10) Zhang, G. D.; Chen, X.; Zhao, Y. R.; Xie, Y. Z.; Qiu, H. Y. *J Phys Chem B* **2007**, *111*, 11708.
(11) Zhao, Y. R.; Chen, X.; Jing, B.; Wang, X. D.; Ma, F. M. *J Phys Chem B* **2009**, *113*, 983.
(12) Fang, D. W.; Zhang, F.; Jia, R.; Shan, W. J.; Xia, L. X.; Yang, J. Z. *Rsc Adv* **2017**, *7*, 11616.
(13) Zorebski, M.; Zorebski, E.; Dzida, M.; Skowronek, J.; Jezak, S.; Goodrich, P.; Jacquemin, J. *J Phys Chem B* **2016**, *120*, 3569.
(14) Xue, L. J.; Gurung, E. S.; Tamas, G.; Koh, Y. P.; Shadeck, M.; Simon, S. L.; Maroncelli, M.; Quitevis, E. L. *J Chem Eng Data* **2016**, *61*, 1078.
(15) Blesic, M.; Marques, M. H.; Plechkova, N. V.; Seddon, K. R.; Rebelo, L. P. N.; Lopes, A. *Green Chem* **2007**, *9*, 481.
(16) Song, Z. H.; Xin, X.; Shen, J. L.; Zhang, H.; Wang, S. B.; Yang, Y. Z. *Rsc Adv* **2016**, *6*, 2966.
(17) Wei, Y.; Wang, F.; Zhang, Z. Q.; Ren, C. C.; Lin, Y. *J Chem Eng Data* **2014**, *59*, 1120.
(18) Singh, T.; Kumar, A. *J Phys Chem B* **2007**, *111*, 7843.
(19) Wang, H. Y.; Wang, J. J.; Zhang, S. B.; Xuan, X. P. *J Phys Chem B* **2008**, *112*, 16682.
(20) Kamboj, R.; Bharmoria, P.; Chauhan, V.; Singh, G.; Kumar, A.; Singh, S.; Kang, T. S. *Phys Chem Chem Phys* **2014**, *16*, 26040.
(21) Kamboj, R.; Bharmoria, P.; Chauhan, V.; Singh, S.; Kumar, A.; Mithu, V. S.; Kang, T. S. *Langmuir* **2014**, *30*, 15040.
(22) Zhao, Y. R.; Yue, X.; Wang, X. D.; Huang, D. D.; Chen, X. *Colloid Surface A* **2012**, *412*, 90.
(23) Akram, M.; Bhat, I. A.; Kabir-ud-Din *Colloid Surface A* **2016**, *493*, 32.
(24) Sharma, K.; Chauhan, S. *Colloid Surface A* **2014**, *453*, 78.
(25) Naderi, O.; Sadeghi, R. *J Chem Thermodyn* **2016**, *102*, 68.
(26) Kumar, S.; Naqvi, A. Z.; Kabir-ud-Din *Langmuir* **2000**, *16*, 5252.
(27) Junquera, E.; Tardajos, G.; Aicart, E. *Langmuir* **1993**, *9*, 1213.
(28) Cassidy, M. A.; Warr, G. G. *J Phys Chem-Us* **1996**, *100*, 3237.
(29) L.Nitschke, L. H. *Environmental aspects of Surfactants, in*, **2002**.
(30) Mukai, T.; Yoshio, M.; Kato, T.; Yoshizawa, M.; Ohno, H. *Chem Commun* **2005**, 1333.
(31) Shanks, P. C.; Franses, E. I. *J. Phys. Chem.* **1992**, 96 1794.
(32) Ao, M.; Kim, D. *J. Chem. Eng. Data*, **2013**, 58, 1529.
(33) Sues, P. S.; Tuchtenhagen, W.; Blume, J. *J. Phys. Chem.*, **1995**, *99*, 11742.
(34) Vanyur, R.; Biczok, L.; Miskolczy, Z. *Colloid Surface A* **2007**, *299*, 256.

(35) Sastry, N. V.; Singh, D. K. *Langmuir* **2016**, *32*, 10000.
(36) Geng, F.; Liu, J.; Zheng, L. Q.; Yu, L.; Li, Z.; Li, G. Z.; Tung, C. H. *J Chem Eng Data* **2010**, *55*, 147.
(37) Adamson, A. W. *Physical Chemistry of Surfaces*, 1976.
(38) Yousuf, S.; Akram, M.; Kabir-ud-Din *Colloid Surface A* **2014**, *463*, 8.
(39) Turro, N. J.; Yekta, A. *J Am Chem Soc* **1978**, *100*, 5951.
(40) Muller, N. *Langmuir* **1993**, *9*, 96.
(41) Mehta, S. K.; Bhasin, K. K.; Chauhan, R.; Dham, S. *Colloid Surface A* **2005**, *255*, 153.